ISSN 1001-0742
CN 11-2629/X

2012

Volume 24
Number 9

JOURNAL OF ENVIRONMENTAL SCIENCES

ELSEVIER
Science Press

Sponsored by
Research Center for Eco-Environmental Sciences
Chinese Academy of Sciences

JOURNAL OF ENVIRONMENTAL SCIENCES

(http://www.jesc.ac.cn)

Aims and scope

Journal of Environmental Sciences is an international academic journal supervised by Research Center for Eco-Environmental Sciences, Chinese Academy of Sciences. The journal publishes original, peer-reviewed innovative research and valuable findings in environmental sciences. The types of articles published are research article, critical review, rapid communications, and special issues.

The scope of the journal embraces the treatment processes for natural groundwater, municipal, agricultural and industrial water and wastewaters; physical and chemical methods for limitation of pollutants emission into the atmospheric environment; chemical and biological and phytoremediation of contaminated soil; fate and transport of pollutants in environments; toxicological effects of terrorist chemical release on the natural environment and human health; development of environmental catalysts and materials.

For subscription to electronic edition

Elsevier is responsible for subscription of the journal. Please subscribe to the journal via http://www.elsevier.com/locate/jes.

For subscription to print edition

China: Please contact the customer service, Science Press, 16 Donghuangchenggen North Street, Beijing 100717, China. Tel: +86-10-64017032; E-mail: journal@mail.sciencep.com, or the local post office throughout China (domestic postcode: 2-580).

Outside China: Please order the journal from the Elsevier Customer Service Department at the Regional Sales Office nearest you.

Submission declaration

Submission of an article implies that the work described has not been published previously (except in the form of an abstract or as part of a published lecture or academic thesis), that it is not under consideration for publication elsewhere. The submission should be approved by all authors and tacitly or explicitly by the responsible authorities where the work was carried out. If the manuscript accepted, it will not be published elsewhere in the same form, in English or in any other language, including electronically without the written consent of the copyright-holder.

Submission declaration

Submission of the work described has not been published previously (except in the form of an abstract or as part of a published lecture or academic thesis), that it is not under consideration for publication elsewhere. The publication should be approved by all authors and tacitly or explicitly by the responsible authorities where the work was carried out. If the manuscript accepted, it will not be published elsewhere in the same form, in English or in any other language, including electronically without the written consent of the copyright-holder.

Editorial

Authors should submit manuscript online at http://www.jesc.ac.cn. In case of queries, please contact editorial office, Tel: +86-10-62920553, E-mail: jesc@263.net, jesc@rcees.ac.cn. Instruction to authors is available at http://www.jesc.ac.cn.

Copyright

ISSN 1001–0742 **Journal of Environmental Sciences** Vol. 24 No. 9 2012

CONTENTS

Aquatic environment

Atmospheric environment

Terrestrial environment

Environmental health and toxicology

Environmental catalysis and materials

Environmental analytical methods

Serial parameter: CN 11-2629/X*1989*m*184*en*P*23*2012-9

Available online at www.sciencedirect.com
ScienceDirect
Journal of Environmental Sciences 2012, 24(9) 1549–1558
JOURNAL OF ENVIRONMENTAL SCIENCES
ISSN 1001-0742
CN 11-2629/X
www.jesc.ac.cn

Adsorptive removal of hydrophobic organic compounds by carbonaceous adsorbents: A comparative study of waste-polymer-based, coal-based activated carbon, and carbon nanotubes

Fei Lian[1,2], Chun Chang[2], Yang Du[2], Lingyan Zhu[2,*], Baoshan Xing[3], Chang Liu[2]

1. Centre for Research in Ecotoxicology and Environmental Remediation, Institute of Agro-environmental Protection, Ministry of Agriculture, Tianjin 300191, China
2. College of Environmental Science and Engineering, Tianjin Key Laboratory of Environmental Remediation and Pollution Control, Key Laboratory of Pollution Processes and Environmental Criteria, Ministry of Education, Nankai University, Tianjin 300071, China
3. Department of Plant, Soil and Insect Sciences, University of Massachusetts, Amherst, Massachusetts 01003, USA

Received 01 November 2011; revised 18 January 2012; accepted 02 March 2012

Abstract

Adsorption of the hydrophobic organic compounds (HOCs) trichloroethylene (TCE), 1,3-dichlorobenzene (DCB), 1,3-dinitrobenzene (DNB) and γ-hexachlorocyclohexane (HCH) on five different carbonaceous materials was compared. The adsorbents included three polymer-based activated carbons, one coal-based activated carbon (F400) and multiwalled carbon nanotubes (MWNT). The polymer-based activated carbons were prepared using KOH activation from waste polymers: polyvinyl chloride (PVC), polyethyleneterephthalate (PET) and tire rubber (TR). Compared with F400 and MWNT, activated carbons derived from PVC and PET exhibited fast adsorption kinetics and high adsorption capacity toward the HOCs, attributed to their extremely large hydrophobic surface area (2700 m^2/g) and highly mesoporous structures. Adsorption of small-sized TCE was stronger on the tire-rubber-based carbon and F400 resulting from the pore-filling effect. In contrast, due to the molecular sieving effect, their adsorption on HCH was lower. MWNT exhibited the lowest adsorption capacity toward HOCs because of its low surface area and characteristic of aggregating in aqueous solution.

Key words: polymer waste; activated carbon; hydrophobic organic compound; adsorption mechanism
DOI: 10.1016/S1001-0742(11)60984-4

Introduction

With its high chemical stability, extensive porosity and variability of surface properties, activated carbon (AC) has found widespread application in many areas such as capacitors, catalyst supports, battery electrodes, and environmental remediation (Derbyshire et al., 2001). Traditionally, lignocellulosics or coals are the most used raw materials for the production of ACs (Bansal et al., 1988). With the increasing amount of polymer waste around the world, there has been a growing interest in preparing ACs from synthesized polymer waste such as polyacrylonitrile, waste tires and used polymeric resin (Park and Jung, 2002; Ryu et al., 2002; San Miguel et al., 2003; Skodras et al., 2007; Long et al., 2008). ACs derived from synthesized polymers usually exhibit superior structural characteristics compared with those from traditional feedstocks (i.e., biomass and coals) mainly due to their uniform composition, high carbon yield and low ash content (Hayashi et al., 2005; Vázquez-Santos et al., 2008). For example, it is reported that ACs derived from waste polyurethane exhibit higher surface area and more evenly distributed pore size than that derived from coconut shell (Hayashi et al., 2005). AC with high microporosity and large surface area (up to 4000 m^2/g) was obtained by heat treatment of poly(2,6-dimethyl-1,4-phenylene oxide) (Yuan et al., 2008).

Due to their unique properties (e.g., large surface area and uniform pore structure), polymer-based ACs have been investigated for removal of organic pollutants, heavy metals, and CO_2 (Arenillas et al., 2005; Hayashi et al., 2005; Manchón-Vizuete et al., 2005; Murillo et al., 2005; Kartel et al., 2006; Sych et al., 2006; Alexandre-Franco et al., 2007; Almazán-Almazán et al., 2007). However, most of these studies focused on the adsorption of organic vapors and ionic dyes (Hayashi et al., 2005; Murillo et al., 2005; Kartel et al., 2006; Sych et al., 2006; Almazán-Almazán et al., 2007). A few studies examined the adsorption mechanisms of organic compounds with polymer-based ACs in aqueous solutions. A previous study reported that the micropores and acidic O-containing groups of waste-polystyrene-based AC played an important role in the adsorption of dibenzothiophene (Wang et al., 2009). Another study compared the adsorption of phenolic compounds (phenol, 3-aminophenol and 3-chlorophenol) on a polymer-based AC with a commercial sample, suggesting

* Corresponding author. E-mail: zhuly@nankai.edu.cn

that the higher adsorption by polymer-based AC could be attributed to its more basic groups (Yenisoy-Karakas et al., 2004). However, little has been done to systematically investigate the adsorption behaviors considering the physicochemical properties of both adsorbents and adsorbates. The roles of surface area, porosity and surface chemistry of polymer-based ACs as well as molecular size and configuration of adsorbates are not well understood. On the other hand, little research has been conducted to compare the adsorption of hydrophobic organic compounds (HOCs) by polymer-derived ACs with other typical carbonaceous materials such as coal-based ACs and carbon nanotubes.

In the present study, three polymer-based ACs using waste polyvinyl chloride (PVC), polyethyleneterephthalate (PET) and tire rubber (TR) were prepared with KOH activation. Surface area, porosity, and structural properties of these ACs were characterized in detail. The adsorption of HOCs on these polymer-based ACs, a commercial coal-based AC, F400 and MWNT, were compared to investigate the correlation of adsorption with the properties of both adsorbates and adsorbents. Four HOCs with different physicochemical properties, i.e., trichloroethylene (TCE), 1,3-dichlorobenzene (DCB), 1,3-dinitrobenzene (DNB) and γ-hexachlorocyclohexane (HCH), were selected to examine the effect of molecular properties on adsorption. The results would also be useful to assess whether ACs derived from polymer waste are promising adsorbents compared with conventional coal-based ACs and carbon nanotubes.

1 Materials and methods

1.1 Raw materials and adsorbates

Tire rubber (TR) particles (size < 0.5 mm) and PVC pellets in the range of 1–3 mm were purchased from Honglian Rubber Industries (Tianjin, China). PET material was obtained by cutting transparent plastic water bottles into small pieces (< 1 cm^2) using stainless steel scissors. All the tested HOCs were chromatographic grade and purchased from ANPEL Chemical Corp. (Shanghai, China). Their selected properties are presented in Table 1.

1.2 Preparation of adsorbents

KOH activation was used to prepare ACs from waste PVC, PET and TR. Briefly, the raw material was carbonized at 600°C in a nitrogen atmosphere for 1 hr. The carbonized sample was then activated by KOH (1:2, *m*/*m*) in a nitrogen stream at 850°C. The time of activation was optimized to obtain a 50% burn-off for all three samples for comparison (Bóta et al., 1997). It took 120 min in the case of TR and 90 min for PVC and PET. The obtained samples were washed with 1 mol/L HCl solution and distilled water to remove the ash and decomposed fragments and then dried at 110°C for 24 hr. The obtained solids were ground and passed through a 150 μm sieve. They were labeled as APVC, APET and ATR, respectively. F400, supplied by Calgon Carbon Co. (Tianjin, China), was pulverized and passed through a 150 μm sieve. MWNT was purchased from Nanotech Port Co. (Shenzhen, China); the size of the outer diameter ranged from 10 to 30 nm and the length of carbon nanotubes ranged from 5 to 15 μm.

1.3 Characterization of adsorbents

The surface chemical composition of the adsorbents was determined using an X-ray photoelectron spectrometer (XPS) (VersaProbe PHI 5000, USA). Ash contents were measured by combusting 5 g of the samples in a muffle furnace at 800°C for 4 hr. Nitrogen adsorption-desorption isotherms were measured at 77 K by an AUTOSORB instrument (Quantachrome, USA). High-resolution transmission electron microscopy (HR-TEM) images were obtained using a transmission electron microscope (JEM-2010FEF, JEOL, Japan) with optimal resolution of 2 nm at 300 kV.

1.4 Adsorption experiment

The adsorption experiments were conducted at 25±1°C in 40 mL amber vials equipped with Teflon-lined screw caps. For adsorption kinetics, 10 mg of adsorbent was added in a 40 mL vial, followed by background solution and solutes (spiked at 10 mg/L). The background solution contained 0.01 mol/L $CaCl_2$ in deionized distilled water and 200 mg/L NaN_3 as a bioinhibitor. The vials were shaken on a rotary shaker (150 r/min) and two vials were taken off at predetermined time periods. The mixture was centrifuged at 4000 ×*g* for 10 min. The upper aqueous solution was extracted with hexane to measure the concentrations of the solutes by gas chromatography (GC) coupled with electron-capture detection (ECD). A capillary column (HP 5, 30 m × 0.32 mm, J&W Scientific Columns from Agilent Technologies) was used for the separation. The mass of adsorbed chemicals was calculated from the measured concentration in the solution based on mass balance. Control experiments with no adsorbents in the vials were carried out simultaneously. No measurable change in the solute concentrations was observed in the controls.

Table 1 Selected physical-chemical properties of trichloroethylene (TCE), 1,3-dichlorobenzene (DCB), 1,3-dinitrobenzene (DNB) and γ-hexachlorocyclohexane (HCH)

Organic compounds	MW (g/mol)	S_w (mmol/L)	K_{ow} (L/L)	ρ (g/cm^3)	V_s (cm^3/mol)	MD (Å)
TCE	131.4	8.32	263	1.46	90	6.6 × 6.2 × 3.6
DCB	147.0	0.83	2951	1.29	114	7.4 × 6.7 × 0.2
DNB	168.1	2.88	30.9	1.57	107	8.7 × 7.1 × 1.5
HCH	290.8	0.025	6026	1.87	156	7.9 × 7.0 × 4.9

MW: molecular weight; S_w: aqueous solubility; K_{ow}: *n*-octanol-water partition coefficient; ρ: density; V_s: molar volume; MD: molecular dimensions, calculated from the Chem^{3}D Program. Values of MW, S_w, K_{ow} and ρ were from Schwarzenbach et al., 2003.

For the isotherm experiments, a given amount of adsorbents (1–10 mg), 40 mL of the background solution, and a stock solution of an adsorbate (in methanol) were added into vials to leave minimal headspace. The vials were tumbled at 3 r/min for 7 days to reach apparent equilibration based on the kinetics study above. Then, after 24 hr to allow complete settlement of adsorbents, an aliquot of the upper solution was subjected to GC/ECD analysis to determine the aqueous concentrations. Calibration curves were obtained from control samples receiving the same treatment as the adsorption samples but without the adsorbents.

2 Results

2.1 Characterization of adsorbents

The results of the surface elemental composition and textural parameters of the adsorbents are summarized in Table 2. The majority of heteroatoms such as O, H and N in the raw materials were removed, resulting in a significant increase in the C content of the polymer-derived adsorbents (APVC, APET and ATR). Among the five adsorbents, APET had the lowest surface C content (77.6%) and highest O content (21.7%), thus the highest polarity. MWNT was dominated by graphitized C (96.7%) and had a low O content (2.79%). A substantial mesopore structure was developed in APET and APVC (over 73% mesoporous), while ATR and F400 were dominated by micropores and mesopores, and MWNT showed more heterogeneous characteristics. Figure 1 illustrates the pore size distribution of the polymer-based adsorbents. APVC displayed a more narrow distribution (2–3 nm) than APET and ATR. The BET surface area (S_{BET}) of APVC and APET was as high as 2666 and 2831 m^2/g, respectively, much larger than that of ATR, F400 and MWNT. The HR-TEM images (Fig. 2) illustrate that just like F400, the polymer based ACs mainly consisted of short stacks of small-sized graphite sheets arranged in a highly disordered fashion.

Table 2 Surface elemental composition and textural parameters of the adsorbents

Adsorbent	Surface elemental composition[a] (dry weight based)					Ash content	S_{BET}[b]	V_{tot}[c]	DFT cumulative pore volume[d] (cm^3/g)				
	C (%)	H (%)	O (%)	N (%)	(O+N)/C	(%)	(m^2/g)	(cm^3/g)	< 7 Å	< 10 Å	< 20 Å	20–500 Å	> 500 Å
APVC	95.4	1.31	3.70	0.50	0.044	5.37	2666	1.44	0.00	0.03	0.25	1.06	0.13
APET	77.6	1.76	21.7	0.52	0.286	1.17	2831	1.68	0.00	0.04	0.25	1.30	0.13
ATR	87.5	2.01	10.3	0.43	0.123	10.5	398	0.38	0.03	0.08	0.12	0.16	0.10
F400	79.1	3.30	16.9	0.65	0.222	8.5	1003	0.52	0.07	0.11	0.25	0.24	0.03
MWNT	96.7	0.00	2.79	0.31	0.032	0.01	162	0.31	0.03	0.04	0.08	0.15	0.08

[a] Determined by X-ray photoelectron spectroscopy (XPS); [b] determined by N_2 adsorption using the Brunauer-Emmett-Teller (BET) method; [c] V_{tot}: total pore volume, determined at $P/P^0 = 0.97$; [d] cumulative pore volume, derived from the Density Functional Theory (DFT).

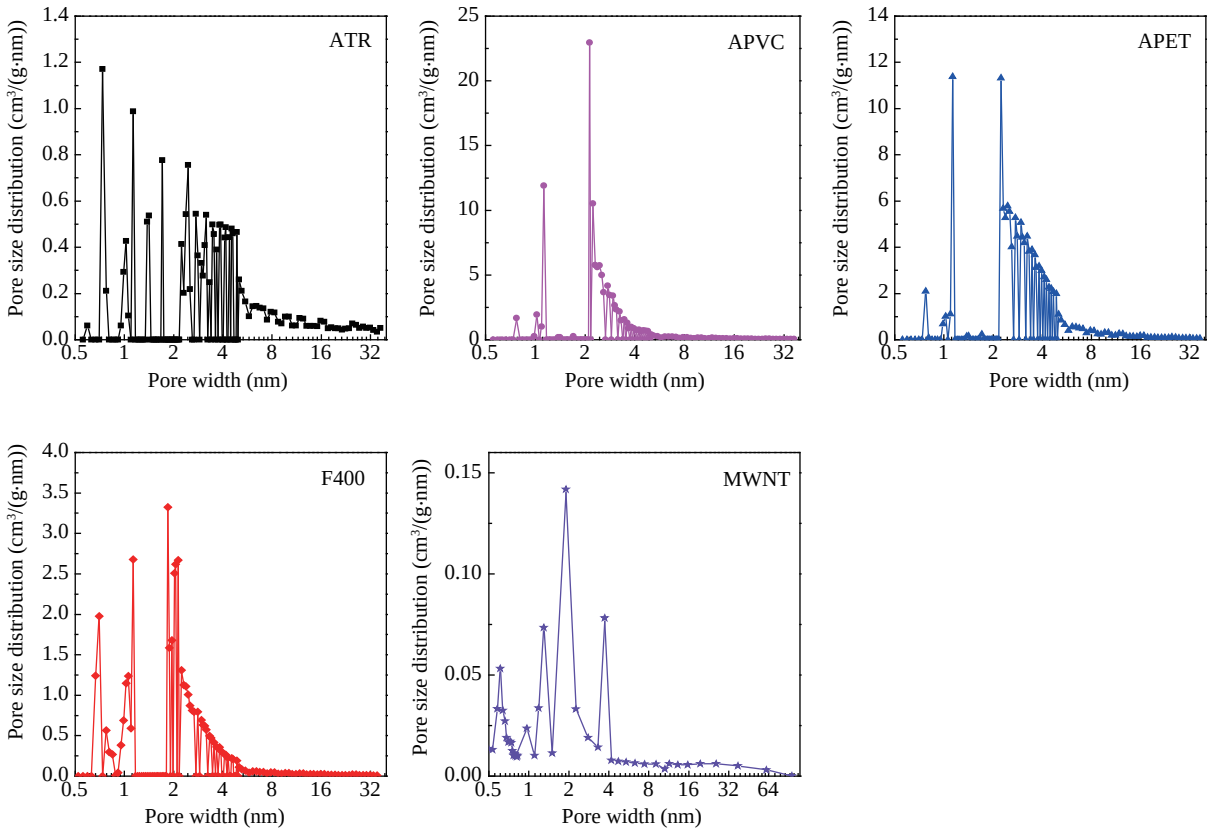

Fig. 1 Pore size distribution of the five carbon adsorbents using density functional theory.

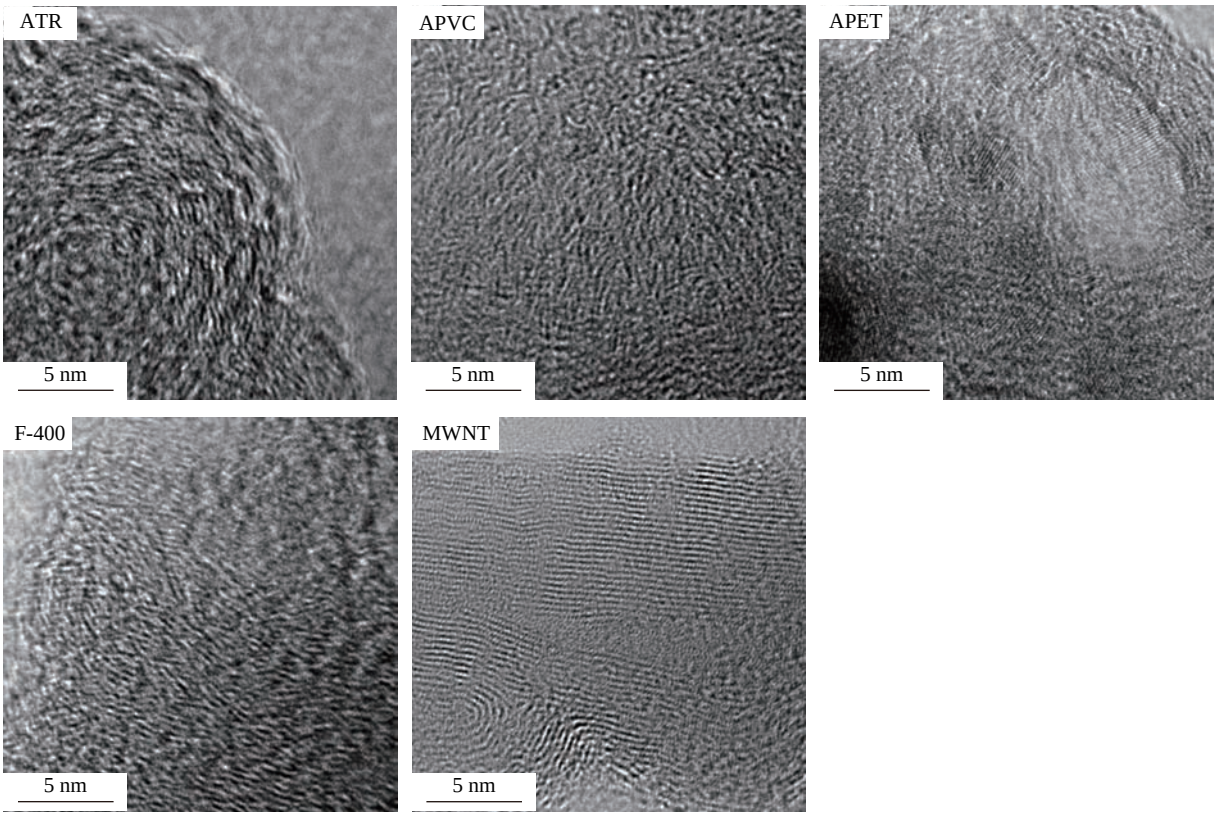

Fig. 2 Representative TEM images of the five carbon adsorbents.

2.2 Adsorption kinetics

Figure 3 compares the adsorption kinetics of the solutes on the five adsorbents. For a given adsorbate, a faster adsorption was observed on the highly mesoporous APVC and APET. Taking DCB as an example, approximately 68% and 62% of the adsorption was accomplished within 1 hr on APVC and APET, while only about 38%, 41% and 44% was adsorbed on ATR, F400 and MWNT, respectively. APVC and APET have a mesoporous structure with narrow pore size distribution (Table 2), thus facilitating the transport of solute molecules into the pores. In contrast, the pore sizes of ATR and F400 are heterogeneous; while carbon nanotubes tend to entangle and aggregate into bundles in aqueous solution, restricting the access of solute molecules into pores (Ji et al., 2010). As a result, diffusion of solutes to the pores of ATR, F400 and MWNT becomes much difficult. The results indicate that the high mesoporosity of APET and APVC makes them more efficient for the uptake of HOCs in aqueous solutions than ATR, F400 and MWNT.

To quantitatively compare the apparent adsorption kinetics between different adsorbents, the pseudo first-order (Eq. (1)), pseudo second-order (Eq. (2)) and intraparticle diffusion (Eq. (3)) (Weber and Morris, 1962) models were used to fit the kinetic data by linear regression.

$$\ln(q_e - q_t) = \ln(q_e) - k_1 t \quad (1)$$

$$\frac{t}{q_t} = \frac{1}{k_2 q_e^2} + \frac{t}{q_e} \quad (2)$$

$$q_t = k_{ip} t^{\frac{1}{2}} + C \quad (3)$$

where, q_e (mg/g) and q_t (mg/g) are the amounts of solutes adsorbed on adsorbents at equilibrium and time t, respectively; k_1 (min^{-1}) and k_2 (g/(mg·hr)) are the equilibrium rate constants of the pseudo first- and second-order models; k_{ip} (mg/(g·$hr^{0.5}$)) is the intraparticle diffusion rate constant and C (mg/g) is a constant that gives information about the thickness of the boundary layer. Only the pseudo second-order model provided the best fitting for all the experiment data with $r^2 > 0.99$ (Table S1). For APVC and APET, the calculated rate constant (k_2) follows an order of TCE > DCB > DNB > HCH, which inversely correlates with the molecular size of the adsorbate (Table 1). Apparently, the results are largely correlated with the porous structure of the adsorbents and adsorbate properties, indicating that the pore diffusion mechanism may play a dominant role in the adsorption kinetics. A similar observation of HOC adsorption by zeolite-templated carbon was reported in a previous study (Ji et al., 2009).

2.3 Adsorption isotherms

Figure 4 illustrates the adsorption isotherms of the solutes on the five adsorbents. The data were fitted with the Freundlich model ($q = K_f C_e^n$), where q (mmol/kg) and C_e (mmol/L) are the solid- and liquid-phase concentrations at adsorption equilibrium; K_f ($mmo1^{1-n}L^n$/kg) is the affinity coefficient, n is the Freundlich linearity index. All the isotherms could be fitted well by the Freundlich model in the tested concentration ranges and the fitting parameters are listed in Table S2. For all the adsorbent/adsorbate combinations, nonlinear isotherms are displayed with

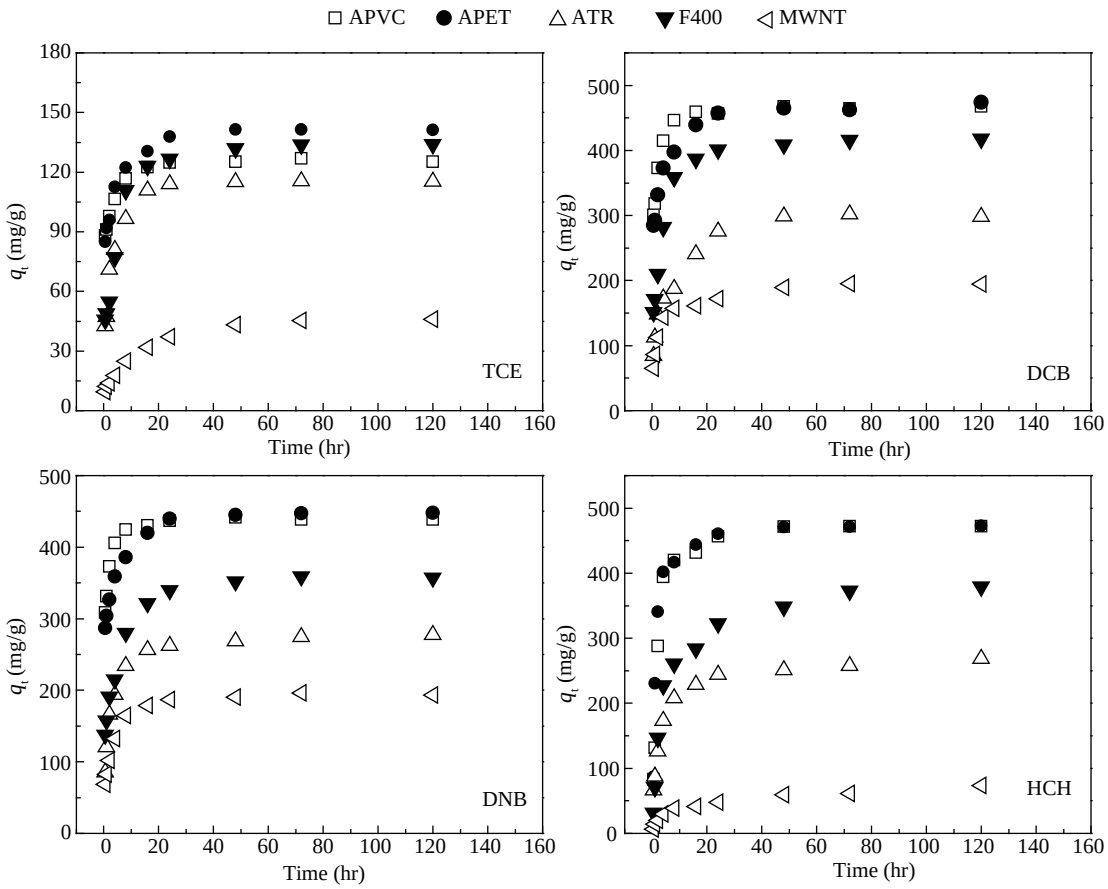

Fig. 3 Adsorption kinetics of TCE, DCB, DNB and HCH on the five carbon adsorbents.

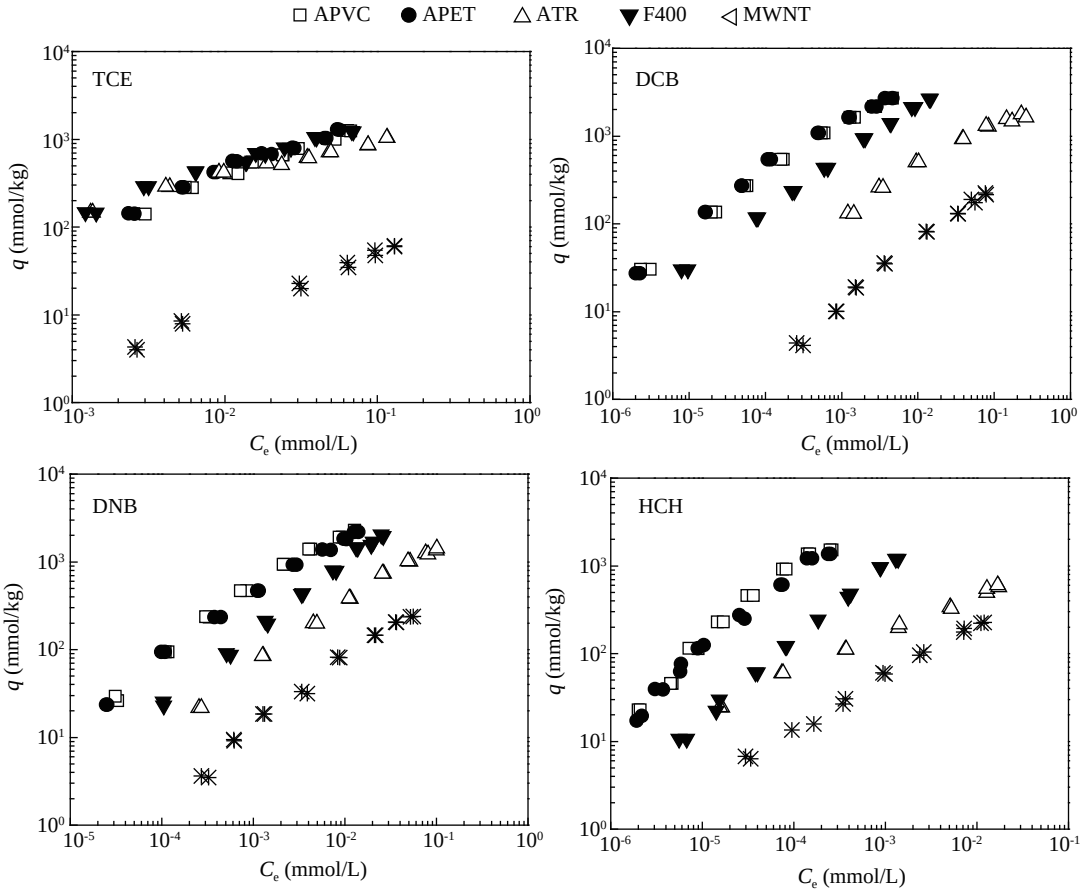

Fig. 4 Adsorption isotherms plotted as adsorbed vs. aqueous concentrations at equilibrium for the five adsorbents.

n from 0.385 to 0.790. The strong nonlinearity (departure of n from 1) is mainly attributed to the adsorption in hydrophobic nanopores and the heterogeneous distribution of adsorption sites on the carbon surface. The adsorption affinity roughly follows the order: APET ≈ APVC > F400 > ATR > MWNT, correlating well with the adsorbent surface area (Table 2). Their large surface area and well-developed mesoporous structure make APET and APVC promising adsorbents for removal of HOCs from contaminated water. Even though APET exhibits much higher surface polarity than APVC, it displays similar or slightly higher adsorption capacity toward the HOCs irrespective of their properties. This is inconsistent with the observation that surface chemistry may overwhelm pore structure effects in HOC adsorption by ACs as reported by Karanfil and Kilduff (1999). The BET surface areas of APVC and APET are up to 2600 and 2800 m^2/g, 2–4 times larger than that of adsorbents used in the study of Karanfil and Kilduff (1999). This suggests that the larger surface area of APET partly compensates for the disadvantageous effect of O-containing polar groups and enables comparable adsorption capacity relative to APVC.

3 Discussion

The impact of adsorbent porosity on the HOC adsorption can be better illustrated by comparing isotherms normalized by surface area (Fig. 5). The normalized adsorption of TCE was much higher on ATR and F400; however, that of HCH was lower on ATR and F400, implying the importance of structural characteristics of adsorbents and adsorbates. For ATR and F400, nitrogen adsorption results indicate that approximate 21% of their pores are less than 10 Å (Table 2). TCE has a planar shape with molecular dimensions of 6.6 Å × 6.2 Å × 3.6 Å (Table 1). It is suggested that planar TCE molecules can access the deep portions of micropores (< 7 Å) in a flat form, and pores with width less than 10 Å are crucial for TCE adsorption (Karanfil and Dastgheib, 2004). Thus, the larger normalized adsorption of TCE on ATR and F400 could be attributed to the pore-filling effect, which greatly enhances the adsorption through overlapping adsorption potentials of opposite pore walls when the adsorbate molecular dimension is close to the pore size (Dubinin, 1975). Contrary to ATR and F400, the pores less than 10 Å in APVC and APET are only around 2% of the total pore volumes (Table 2) and most micropores are much larger than the molecular size of TCE. Thus the pore-filling effect is insignificant by comparison. On the other hand, the molecular dimensions of HCH are 7.9 Å × 7.0 Å × 4.9 Å (Table 1), much larger than TCE. Thus a large portion of micropores cannot be accessed by HCH molecules. More than 73% of the pores in APVC and APET are mesopores (> 20 Å), which are available for HCH, and the molecular sieving effect is less prominent compared with ATR and F400 (Fig. 5). Moreover, it was suggested that the micropores of ACs mainly consist of slit pores while mesopores exhibit both slit-like and rounded/elongated morphologies, which has been supported by scanning tunneling microscopy analysis (Paredes et al., 2006). Thus it is more difficult for nonplanar HCH molecules to enter into micropores relative to those molecules with similar size but having a planar structure. Similarly, in the adsorption kinetics, diffusion of HCH within the very narrowly distributed and slightly larger-sized pores of APVC becomes relatively slower as evidenced by the lower rate constant (k_2) (Table S1). In contrast, the fast adsorption kinetics of HCH observed on ATR, F400 and MWNT could be due to the size-exclusion effect (Ji et al., 2010). Owing to the high microporosity of ATR and F400, HCH molecules cannot enter the micropores and the adsorption is expected to occur mainly on the external surface, thus shortening the adsorption process. It is worth noting that APVC shares a similar BET surface area and pore structure with APET, however, the rate constant (k_2) is much higher than APET except for adsorption of HCH. This may be attributed to the fact that APET has much higher polarity than APVC, revealed by the surface (O+N)/C molar ratio (Table 2). The O-containing polar groups facilitate the formation of water molecule clusters on the surface of the adsorbent, impeding the diffusion of HOCs into inner pores (Chun et al., 2004).

To further illustrate the correlation of the adsorption of HOCs with adsorbent porosity and adsorbate properties, adsorption data were fitted with the Polanyi-Dubinin-Manes (PDM) model (Eq. (4)), which is applicable for both surface area and pore-filling adsorption mechanisms (Yang et al., 2006).

$$\log q = \log Q^0 + \alpha \left[\frac{RT \ln\left(\frac{C_s}{C_e}\right)}{V_s} \right]^b \quad (4)$$

where, Q^0 (mmol/kg) is the maximum adsorption capacity of the adsorbate; α and b are adsorption constants; V_s is the molar volume of solute; R (8.314×10^{-3} kJ/(mol·K)) is the universal gas constant, T (K) is absolute temperature, and C_s stands for solubility at 20°C.

The PDM model fits the adsorption data quite well in the tested concentration ranges with r^2 0.977–0.999 (Table S2). The surface monolayer coverage (Q_m, mmol/kg) of the solutes on the adsorbents was calculated using the following equation: $Q_m = S/A \cdot N_A$, where S (m^2/g) is the specific surface area of adsorbent, A (nm^2) is the adsorbed cross-section area of an adsorbate molecule (Table 1) and N_A (mol^{-1}) is Avogadro's number. The maximum adsorption capacity (Q^0) was derived from the PDM model (Table S2), and the ratio of Q^0 and Q_m (R_Q) is presented in Fig. 6. For a given adsorbate on APVC and APET, R_Q < 1, implying that monolayer adsorption of the adsorbates could only partially cover the surface of the two adsorbents in the experimental C_e ranges. As for ATR and F400, however, the ratio R_Q is larger than 1 for TCE, DCB and DNB except for HCH, suggesting that multilayer adsorption occurs in the adsorption of TCE, DCB and DNB by ATR and F400; while for HCH, only 59% and 80% of the surface of ATR and F400 is covered, strongly supporting the presence of the molecular sieving effect. Similar results were observed for MWNT, indicating that

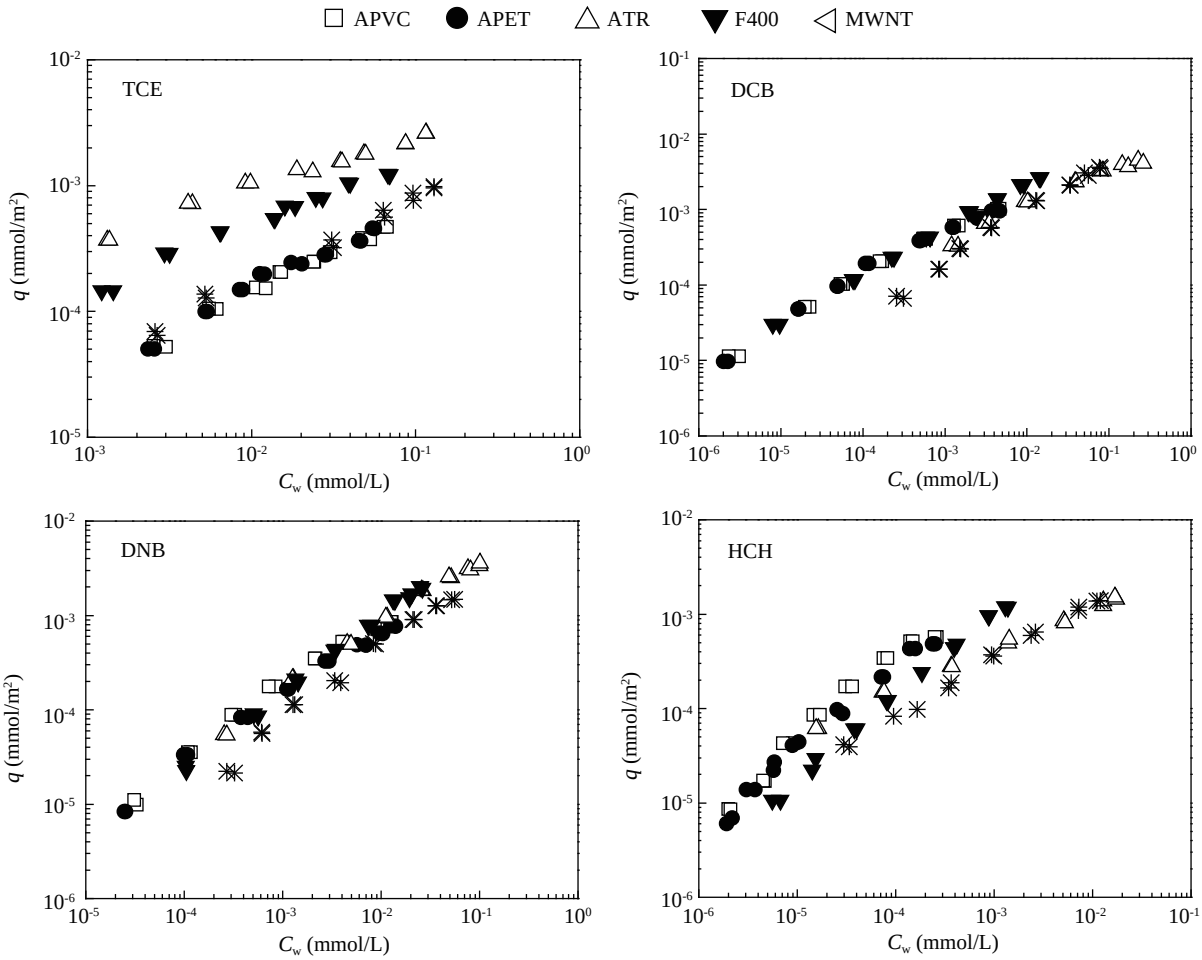

Fig. 5 Adsorption isotherms plotted as adsorbed concentrations normalized to surface area vs. aqueous concentrations at equilibrium for the five adsorbents.

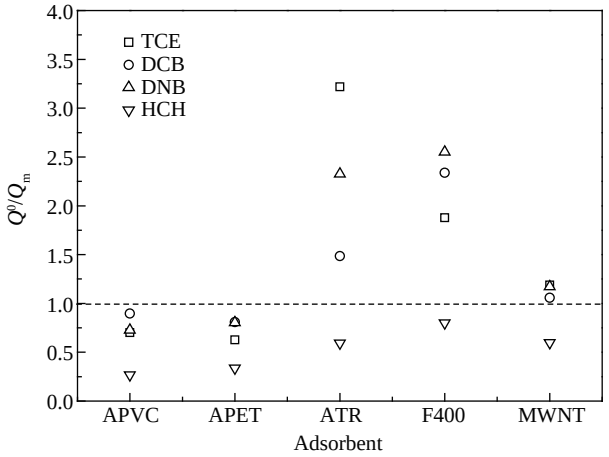

Fig. 6 Ratio between estimated adsorption capacities, Q^0, from the PDM model and calculated monolayer adsorption capacities, Q_m.

large molecules (e.g. HCH) may not be able to access the adsorption sites inside the aggregates of bundled MWNT in aqueous solution. A similar observation was reported in the adsorption of dialkyl phthalate esters on MWNT (Wang et al., 2010). In fact, one of the main shortcomings of using microporous ACs and carbon nanotubes as adsorbents in water treatment is the low adsorption capacity for bulky molecules due to the size-exclusion effect.

The adsorptive interactions were examined by comparing the adsorption isotherms of TCE, DCB, DNB and HCH on each adsorbent directly. Among the adsorbates, TCE and HCH are nonpolar aliphatics, which implies that there is negligible specific interaction with the carbon surface of the adsorbents. Within the tested concentration ranges, the adsorption coefficients (K_d) of HCH are much higher than those of TCE on the same adsorbents. For example, the K_d on APVC is in the order of 10^6–10^7 L/kg for HCH and 10^4 L/kg for TCE, which could be due to the higher hydrophobicity of HCH relative to TCE (indexed by $\log K_{ow}$, Table 1). It has been demonstrated that hydrophobicity plays an important role in HOC adsorption on carbon adsorbents (Yang et al., 2006; Wang and Xing, 2007). However, despite the much lower hydrophobicity, DNB exhibits a K_d comparable to DCB, implying that other specific interaction(s) may promote DNB's adsorption. For a deeper insight into the structure-dependent specific interaction(s), the adsorption affinity was normalized with the corresponding K_{ow} to account for the contribution of hydrophobicity. It can be seen from Fig. 7 that the normalized adsorption affinities of TCE, DCB and HCH to APVC, APET and MWNT are very close to each other while much lower than that of DNB. Likewise, previous studies revealed that nitroaromatic compounds could adsorb strongly from aqueous solution to carbonaceous materials (e.g., carbon nanotubes and biochars) (Zhu et al., 2005;

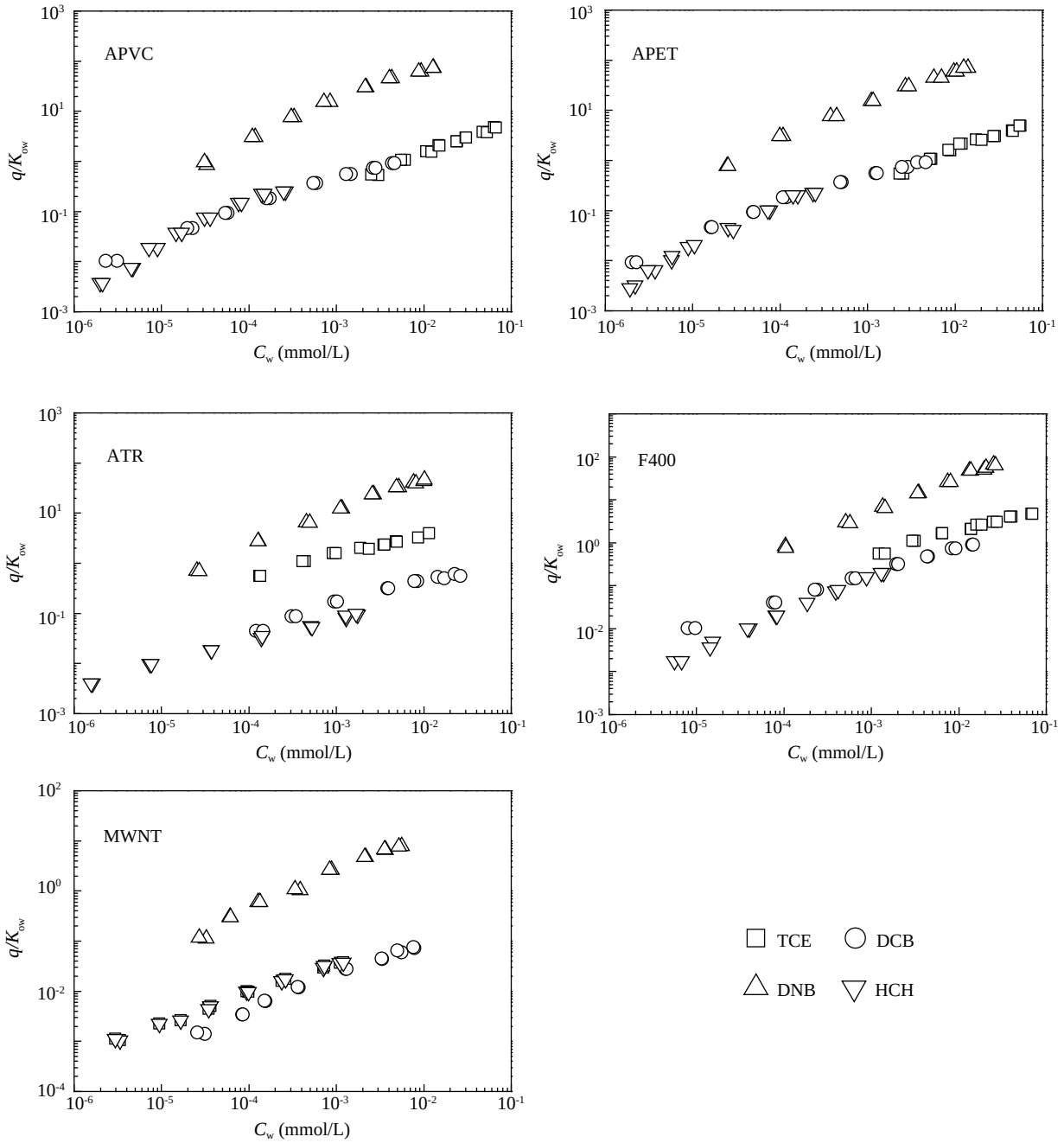

Fig. 7 K_{ow} normalized adsorption isotherms of TCE, DCB, DNB and HCH on the five adsorbents.

Chen et al., 2007; Ji et al., 2009). Nitroaromatics are highly polar and often act as strong electron acceptors when interacting with adsorbents with high electron polarizability. It was proposed that a specific π-π electron-donor-acceptor (EDA) complex is formed when nitroaromatics, which are electron-deficient and act as π acceptors, are adsorbed on the graphene surface of carbons (π donors) (Zhu et al., 2004). The polymer-derived adsorbents (APVC, APET and ATR) consist of stacks of graphene sheets arranged in a highly disordered manner as reflected by the HR-TEM images (Fig. 2). They contain polarized π-electron-rich and π-electron-depleted regions due to surface defects. The graphene surface of MWNT is highly polarizable and can act as an effective electron donor (Chen et al., 2007). Thus, the high adsorption affinity of DNB in this study could be attributed to the EDA interactions between DNB and the graphene sheets of adsorbents.

4 Conclusions

The adsorption of HOCs on ACs derived from three waste polymers were compared with a commercial coal-based AC (F400), and MWNT. The high surface area (up to 2700 m^2/g), mesoporous structure, and narrow pore size distribution make carbons derived from waste PVC and PET superior adsorbents for HOCs in wastewater treatment, in particular the bulky ones, compared to the commercial microporous AC and MWNT. For bulky chemicals, F400 and MWNT may be not effective adsorbents due to the molecular sieving effect and slow adsorption kinetics

resulting from the highly heterogeneous pore structure. On the other hand, the significant discrepancy in pore structure and surface chemistry of the three ACs based on waste polymers indicated that the parent polymers may play a crucial role in the properties of the obtained ACs. Therefore, raw polymers should be precisely selected to improve the HOCs adsorption efficiency of the waste-polymer-derived ACs.

Acknowledgment

This work was supported by the Tianjin Municipal Science and Technology Commission (No. 08ZCGHHZ01000), the Ministry of Education of China (No. 708020), the Ministry of Science and Technology of China (No. 2008ZX08526-003, 2009DFA91910), the New Century Talent program, and the China-US Center for Environmental Remediation and Sustainable Development.

Supporting materials

Adsorption kinetic parameters of pseudo first-order, pseudo second-order and intraparticle diffusion models. Freundlich and PDM model parameters for the HOC adsorption.

References

Alexandre-Franco M, Fernández-González C, Macías-García A, Gómez-Serrano V, 2007. Uptake of lead by carbonaceous adsorbents developed from tire rubber. *Adsorption*, 14(4-5): 591–600.

Almazán-Almazán M C, Pérez-Mendoza M, López-Domingo F J, Fernández-Morales I, Domingo-Garía M, López-Garzón F J, 2007. A new method to obtain microporous carbons from PET: Characterisation by adsorption and molecular simulation. *Microporous and Mesoporous Materials*, 106(1-3): 219–228.

Arenillas A, Rubiera F, Parra J B, Ania C O, Pis J J, 2005. Surface modification of low cost carbons for their application in the environmental protection. *Applied Surface Science*, 252(3): 619–624.

Bansal R C, Donet B J, Stoeckli F, 1988. Active Carbon. Marcel Dekker, New York.

Bóta A, László K, Nagy L G, Copitzky T, 1997. Comparative study of active carbons from different precursors. *Langmuir*, 13(24): 6502–6509.

Chen W, Duan L, Zhu D Q, 2007. Adsorption of polar and nonpolar organic chemicals to carbon nanotubes. *Environmental Science & Technology*, 41(24): 8295–8300.

Chun Y, Sheng G Y, Chiou C T, Xing B S, 2004. Compositions and sorptive properties of crop residue-derived chars. *Environmental Science & Technology*, 38(17): 4649–4655.

Derbyshire F, Jagtoyen M, Andrews R, Rao A, Martín-Gullón I, Grulke E, 2001. Carbon Materials in Environmental Applications. Marcel Decker, New York.

Dubinin M M, 1975. Porous structure and adsorption properties of active carbons. In: Chmistry and Physics of Carbon (Walker P L, ed.). Marcel Dekker, New York. 2: 51–120.

Hayashi J, Yamamoto N, Horikawa T, Muroyama K, Gomes V G, 2005. Preparation and characterization of high-specific-surface-area activated carbons from K_2CO_3-treated waste polyurethane. *Journal of Colloid and Interface Science*, 281(2): 437–443.

Ji L L, Liu F L, Xu Z Y, Zheng S R, Zhu D Q, 2009. Zeolite-templated microporous carbon as a superior adsorbent for removal of monoaromatic compounds from aqueous solution. *Environmental Science & Technology*, 43(20): 7870–7876.

Ji L L, Liu F L, Xu Z Y, Zheng S R, Zhu D Q, 2010. Adsorption of pharmaceutical antibiotics on template-synthesized ordered micro- and mesoporous carbons. *Environmental Science & Technology*, 44(8): 3116–3122.

Karanfil T, Dastgheib S A, 2004. Trichloroethylene adsorption by fibrous and granular activated carbons: Aqueous phase, gas phase, and water vapor adsorption studies. *Environmental Science & Technology*, 38(22): 5834–5841.

Karanfil T, Kilduff J E, 1999. Role of granular activated carbon surface chemistry on the adsorption of organic compounds. 1. Priority pollutants. *Environmental Science & Technology*, 33(18): 3217–3224.

Kartel M T, Sych N V, Tsyba M M, Strelko V V, 2006. Preparation of porous carbons by chemical activation of polyethyleneterephthalate. *Carbon*, 44(5): 1019–1022.

Long C, Lu J D, Li A M, Hu D B, Liu F Q, Zhang Q X, 2008. Adsorption of naphthalene onto the carbon adsorbent from waste ion exchange resin: Equilibrium and kinetic characteristics. *Journal of Hazardous Materials*, 150(3): 656–661.

Manchón-Vizuete E, Macías-García A, Gisbert A N, Fernández-González C, Gómez-Serrano V, 2005. Adsorption of mercury by carbonaceous adsorbents prepared from rubber of tyre wastes. *Journal of Hazardous Materials*, 119(1-3): 231–238.

Murillo R, Navarro M V, García T, López J M, Callén M S, Aylón E et al., 2005. Production and application of activated carbons made from waste tire. *Industrial & Engineering Chemistry Research*, 44(18): 7228–7233.

Paredes J I, Martínez-Alonso A, Hou P X, Kyotani T, Tascón J M D, 2006. Imaging the structure and porosity of active carbons by scanning tunneling microscopy. *Carbon*, 44(12): 2469–2478.

Park S J, Jung W Y, 2002. Preparation and structural characterization of activated carbons based on polymeric resin. *Journal of Colloid and Interface Science*, 250(1): 196–200.

Ryu Z Y, Rong H Q, Zheng J T, Wang M Z, Zhang B J, 2002. Microstructure and chemical analysis of PAN-based activated carbon fibers prepared by different activation methods. *Carbon*, 40(7): 1144–1147.

San Miguel G, Fowler G D, Sollars C J, 2003. A study of the characteristics of activated carbons produced by steam and carbon dioxide activation of waste tyre rubber. *Carbon*, 41(5): 1009–1016.

Schwarzenbach R P, Gschwend P M, Imboden D M, 2003. Environmental Organic Chemistry (2nd ed.). Wiley Interscience, New York.

Skodras G, Diamantopouiou I, Zabaniotou A, Stavropoulos G, Sakellaropoulos G P, 2007. Enhanced mercury adsorption in activated carbons from biomass materials and waste tires. *Fuel Processing Technology*, 88(8): 749–758.

Sych N V, Kartel N T, Tsyba N N, Strelko V V, 2006. Effect of combined activation on the preparation of high porous active carbons from granulated post-consumer polyethyleneterephthalate. *Applied Surface Science*, 252(23): 8062–8066.

Vázquez-Santos M B, Castro-Muñiz A, Martínez-Alonso A, Tascón J M D, 2008. Porous texture evolution in activated

carbon fibers prepared from poly (p-phenylene benzobisoxazole) by carbon dioxide activation. *Microporous and Mesoporous Materials*, 116(1-3): 622–626.

Wang F, Yao J, Sun K, Xing B S, 2010. Adsorption of dialkyl phthalate esters on carbon nanotubes. *Environmental Science & Technology*, 44(18): 6985–6991.

Wang Q, Liang X Y, Qiao W M, Liu C J, Liu X J, Zhan L A et al., 2009. Preparation of polystyrene-based activated carbon spheres with high surface area and their adsorption to dibenzothiophene. *Fuel Processing Technology*, 90(3): 381–387.

Wang X L, Xing B S, 2007. Sorption of organic contaminants by biopolymer-derived chars. *Environmental Science & Technology*, 41(24): 8342–8348.

Weber W J, Morris J C, 1962. Proceedings of the International Conference on Water Pollution Symposium. Pergamon Press, Oxford.

Yang K, Zhu L Z, Xing B S, 2006. Adsorption of polycyclic aromatic hydrocarbons by carbon nanomaterials. *Environmental Science & Technology*, 40(6): 1855–1861.

Yenisoy-Karakas S, Aygün A, Günes M, Tahtasakal E, 2004. Physical and chemical characteristics of polymer-based spherical activated carbon and its ability to adsorb organics. *Carbon*, 42(3): 477–484.

Yuan Y X, Cabasso I, Liu H, 2008. Surface morphology of nanostructured polymer-based activated carbons. *Journal of Physical Chemistry B*, 112(46): 14364–14372.

Zhu D Q, Hyun S H, Pignatello J J, Lee L S, 2004. Evidence for pi-pi electron donor-acceptor interactions between pi-donor aromatic compounds and pi-acceptor sites in soil organic matter through pH effects on sorption. *Environmental Science & Technology*, 38(16): 4361–4368.

Zhu D Q, Kwon S, Pignatello J J, 2005. Adsorption of single-ring organic compounds to wood charcoals prepared under different thermochemical conditions. *Environmental Science & Technology*, 39(11): 3990–3998.

Supporting materials

Table S1 Adsorption kinetic parameters of pseudo-first-order, pseudo-second-order and intraparticle diffusion models for TCE, DCB, DNB and HCH adsorption on the polymer derived adsorbents (APVC, APET and ATR), commercial activated carbon (F400), and multi-walled carbon nanotubes (MWNT)

Solute	Adsorbent	q_{exp}[a] (mg/g)	Pseudo-first order model			Pseudo-second order model			Intraparticle diffusion model		
			q_e[b] (mg/g)	k_1 (min^{-1})	r^2	q_e[b] (mg/g)	k_2 (g/(mg·hr))	r^2	k_{ip} (mg /(g·hr0.5))	C (mg/g)	r^2
TCE	APVC	125.2	118.1	3.4×10^{-2}	0.466	126.1	1.9×10^{-2}	0.999	3.59	96.92	0.624
	APET	168.9	129.8	2.3×10^{-2}	0.521	142.7	8.1×10^{-3}	1.000	5.49	96.31	0.702
	ATR	115.2	110.3	8.4×10^{-3}	0.882	117.4	4.9×10^{-3}	0.999	5.93	67.56	0.650
	F400	134.0	128.6	5.0×10^{-3}	0.884	136.6	3.6×10^{-3}	1.000	9.12	59.27	0.671
	MWNT	45.9	43.0	2.0×10^{-3}	0.889	47.92	3.9×10^{-3}	0.997	3.88	11.34	0.876
DCB	APVC	467.6	446.4	2.7×10^{-2}	0.670	469.5	4.8×10^{-3}	0.998	13.9	356.8	0.516
	APET	474.2	430.5	2.3×10^{-2}	0.535	476.2	2.0×10^{-3}	0.997	18.2	318.8	0.711
	ATR	298.3	274.4	5.1×10^{-3}	0.786	307.7	1.2×10^{-3}	0.998	9.68	219.0	0.689
	F400	418.3	398.8	7.0×10^{-3}	0.886	423.7	1.5×10^{-3}	1.000	17.3	274.0	0.638
	MWNT	194.2	176.7	9.6×10^{-3}	0.867	197.6	2.6×10^{-3}	0.999	11.3	98.99	0.700
DNB	APVC	438.5	423.1	3.5×10^{-2}	0.684	440.0	8.7×10^{-3}	0.999	10.3	358.3	0.486
	APET	448.1	411.3	2.8×10^{-2}	0.479	451.3	2.8×10^{-3}	0.998	15.7	318.4	0.713
	ATR	277.5	260.5	8.5×10^{-3}	0.919	280.1	2.4×10^{-3}	0.997	7.49	211.9	0.744
	F400	357.3	332.9	7.3×10^{-3}	0.771	363.6	1.5×10^{-3}	0.999	18.0	208.2	0.716
	MWNT	193.2	184.4	7.4×10^{-3}	0.884	196.7	3.5×10^{-3}	0.999	11.7	98.72	0.645
HCH	APVC	472.4	458.7	7.2×10^{-3}	0.979	480.8	1.3×10^{-3}	0.998	30.7	229.3	0.478
	APET	472.7	456.1	0.1×10^{-3}	0.967	478.5	1.8×10^{-3}	0.997	26.0	267.3	0.435
	ATR	268.7	246.0	5.8×10^{-3}	0.941	271.0	1.5×10^{-3}	0.999	18.1	113.1	0.685
	F400	379.4	343.0	3.8×10^{-3}	0.945	392.2	1.6×10^{-3}	0.999	31.1	110.2	0.726
	MWNT	73.3	60.32	2.1×10^{-3}	0.862	74.0	1.6×10^{-3}	0.984	6.00	13.24	0.911

[a] Equilibrium adsorbed concentration measured from batch experiments; [b] equilibrium adsorbed concentrations calculated from pseudo first and second-order models, respectively

Table S2 Freundlich and PDM model parameters for adsorption of HOCs to polymer derived adsorbents (APVC, APET and ATR), commercial activated carbon (F400), and multi-walled carbon nanotubes (MWNT)

Chemical	Adsorbent	Freundlich model				PDM model			
		K_f ($mmol^{1-n}L^n/kg$)	n	R^2	Q^{0a} (mmol/kg)	a	b	R^2	Q_m[b] (mmol/kg)
TCE	APVC	6500 ± 440	0.611 ± 0.02	0.990	7610 ± 530	–15.8 ± 8.25	1.48 ± 0.44	0.990	10800
	APET	6800 ± 680	0.668 ± 0.02	0.978	7200 ± 740	–16.0 ± 13.5	1.54 ± 0.73	0.977	11500
	ATR	2300 ± 100	0.389 ± 0.01	0.988	5150 ± 664	–5.58 ± 1.36	0.88 ± 0.33	0.987	1600
	F400	4600 ± 300	0.475 ± 0.02	0.985	7700 ± 122	–17.0 ± 8.01	1.77 ± 0.38	0.988	4100
	MWNT	248 ± 24	0.688 ± 0.04	0.988	780 ± 50.1	–9.06 ± 3.18	0.78 ± 0.50	0.987	657
DCB	APVC	36000 ± 3000	0.476 ± 0.01	0.996	7970 ± 985	–26.1 ± 5.13	1.84 ± 0.14	0.999	8900
	APET	32000 ± 3500	0.454 ± 0.02	0.992	7600 ± 1880	–23.9 ± 9.35	1.83 ± 0.28	0.995	9400
	ATR	3100 ± 200	0.385 ± 0.03	0.969	1930 ± 97.5	–41.1 ± 16.7	1.81 ± 0.18	0.990	1300
	F400	29000 ± 1800	0.554 ± 0.03	0.996	7720 ± 1800	–22.3 ± 5.20	1.52 ± 0.15	0.998	3300
	MWNT	1000 ± 70	0.599 ± 0.02	0.992	574 ± 148	–19.8 ± 7.82	1.30 ± 0.22	0.993	543
DNB	APVC	25000 ± 2600	0.543 ± 0.02	0.991	5160 ± 563	–67.6 ± 21.4	2.52 ± 0.21	0.998	7100
	APET	29000 ± 2900	0.600 ± 0.02	0.994	6100 ± 526	–56.5 ± 9.03	2.31 ± 0.08	0.994	7600
	ATR	5200 ± 420	0.563 ± 0.03	0.986	2560 ± 311	–67.7 ± 30.9	2.17 ± 0.25	0.997	1100
	F400	29000 ± 4800	0.728 ± 0.04	0.985	6890 ± 3660	–72.8 ± 81.1	2.22 ± 0.69	0.988	2700
	MWNT	1600 ± 160	0.638 ± 0.03	0.989	511 ± 72.1	–95.6 ± 46.3	2.38 ± 0.28	0.997	436
HCH	APVC	260000 ± 115000	0.611 ± 0.05	0.959	2135 ± 236	–7718 ± 1280	4.18 ± 0.77	0.992	8000
	APET	520000 ± 240000	0.705 ± 0.05	0.972	2860 ± 968	–911 ± 1931	3.01 ± 0.99	0.983	8500
	ATR	3400 ± 260	0.436 ± 0.02	0.993	712 ± 39.3	–10.2 ± 2.33	0.94 ± 0.09	0.993	1200
	F400	230000 ± 48900	0.790 ± 0.03	0.993	2400 ± 835	–114 ± 77.4	1.81 ± 0.30	0.996	3000
	MWNT	2700 ± 250	0.555 ± 0.02	0.995	291 ± 13.1	–32.2 ± 7.62	1.29 ± 0.09	0.997	487

[a] The maximum mass sorption capacity, Q^0 was calculated from the PMM model; [b] the monolayer coverage, Q_m was calculated from the surface area of individual sorbents and the molecular surface area of the solute.

JOURNAL OF ENVIRONMENTAL SCIENCES

Journal of Environmental Sciences (Established in 1989)
Vol. 24 No. 9 2012

Supervised by	Chinese Academy of Sciences	**Published by**	Science Press, Beijing, China
Sponsored by	Research Center for Eco-Environmental		Elsevier Limited, The Netherlands
	Sciences, Chinese Academy of Sciences	**Distributed by**	
Edited by	Editorial Office of Journal of	Domestic	Science Press, 16 Donghuangchenggen
	Environmental Sciences (JES)		North Street, Beijing 100717, China
	P. O. Box 2871, Beijing 100085, China		Local Post Offices through China
	Tel: 86-10-62920553; http://www.jesc.ac.cn	Foreign	Elsevier Limited
	E-mail: jesc@263.net, jesc@rcees.ac.cn		http://www.elsevier.com/locate/jes
Editor-in-chief	Hongxiao Tang	**Printed by**	Beijing Beilin Printing House, 100083, China

CN 11-2629/X **Domestic postcode: 2-580** **Domestic price per issue RMB ¥ 110.00**

ISSN 1001-0742